ELSEVIER

J. Non-Newtonian Fluid Mech. 152 (2008) 184–194

Journal of Non-Newtonian Fluid Mechanics

www.elsevier.com/locate/jnnfm

Molecular dynamics simulation of temperature and pressure effects on the intermediate length scale dynamics and zero shear rate viscosity of *cis*-1,4-polybutadiene: Rouse mode analysis and dynamic structure factor spectra

Georgia Tsolou [a,b], Vagelis A. Harmandaris [a,c], Vlasis G. Mavrantzas [a,b,*]

[a] *Institute of Chemical Engineering and High-Temperature Chemical Processes (FORTH-ICE/HT), Patras GR 26504, Greece*
[b] *University of Patras, Department of Chemical Engineering, Patras GR 26504, Greece*
[c] *Max Planck Institute for Polymer Research, D-55128 Mainz, Germany*

Received 29 December 2006; received in revised form 7 August 2007; accepted 4 October 2007

Abstract

A well-relaxed atomistic configuration of a 32-chain C_{128} *cis*-1,4-polybutadiene (*cis*-1,4-PB) system has been subjected to long (on the order of a few microseconds) molecular dynamics (MD) simulations in the NPT ensemble using the united-atom forcefield introduced by Smith et al. [G. Smith, D. Bedrov, W. Paul, A molecular dynamics simulation study of the alpha-relaxation in a 1,4-polybutadiene melt as probed by the coherent dynamic structure factor, J. Chem. Phys. 121 (2004) 4961–4967] on the basis of quantum chemistry calculations. This allowed us to study the temperature and pressure dependences of the Rouse-mode relaxation spectrum of *cis*-1,4-PB over a wide range of temperature (ranging from $T = 430$ K down to 165 K) and pressure (from $P = 1$ atm up to 3.5 kbar) conditions. Results are presented for: (a) the time decay of the autocorrelation function of the normal coordinates (Rouse modes), (b) the single chain intermediate coherent dynamic structure factor, $S_{coh}(q, t)$, and (c) the intermediate incoherent dynamic structure factor, $S_{inc}(q, t)$, for different values of the wavevector q. By mapping our MD simulation results onto the Rouse model, we have been able to extract a prediction for the zero shear rate viscosity of the simulated *cis*-1,4-PB system as a function of temperature and analyze its fragile character. In agreement with our previous MD simulation studies on the same system [G. Tsolou, V.A. Harmandaris, V.G. Mavrantzas, Atomistic molecular dynamics simulation of the temperature and pressure dependences of local and terminal relaxations in *cis*-1,4-polybutadiene, J. Chem. Phys. 124 (2006) 084906-1-11] and in contrast to what is experimentally observed [see, e.g., G. Floudas, T. Reisinger, Pressure dependence of the local and global dynamics of polyisoprene, J. Chem. Phys. 111 (1999) 5201–5204; C.M. Roland, R. Casalini, T. Psurek, S. Pawlus, M. Paluch, Segmental- and normal-mode dielectric relaxation of poly(propylene glycol) under pressure, J. Polym. Sci. Part B: Polym. Phys. 41 (2003) 3047–3052], we predict that pressure and temperature influence practically similarly all normal mode relaxation times along the simulated C_{128} *cis*-1,4-PB chain. Furthermore, our MD simulation results predict a transition from a homogeneous to a heterogeneous dynamical behavior in the region of wavevectors near the first (intermolecular) peak in the static structure factor, consistently with recent neutron scattering (NS) measurements [see, e.g., B. Frick, G. Dosseh, A. Cailliaux, C. Alba-Simionesco, Pressure dependence of the segmental relaxation of polybutadiene and polyisobutylene and influence of molecular weight, Chem. Phys. 292 (2003) 311–323; A. Arbe, J. Colmenero, B. Farago, M. Monkenbusch, U. Buchenau, D. Richter, Intermediate length scale dynamics in glass forming polymers: coherent and incoherent quasielastic neutron scattering results on polyisobutylene, Chem. Phys. 292 (2003) 295–309] and previous simulation studies [see, e.g., J. Colmenero, F. Alvarez, A. Arbe, Self-motion and the alpha relaxation in a simulated glass-forming polymer: Crossover from Gaussian to non-Gaussian dynamic behavior, Phys. Rev. E 65 (2002) 041804-1-12].

Keywords: Rouse modes; Relaxation; Viscosity; Pressure; Temperature; Homogeneous and heterogeneous dynamics; Fragility; Molecular dynamics

1. Introduction

Temperature and pressure effects on the segmental and terminal relaxation properties of polymers such as polyisoprene (PI), polybutadiene (PB), polyisobutylene (PIB) and poly(propylene

* Corresponding author at: University of Patras, Department of Chemical Engineering, Patras GR 26504, Greece. Tel.: +30 2610 997 398; fax: +30 2610 965 223.
E-mail address: vlasis@chemeng.upatras.gr (V.G. Mavrantzas).

0377-0257/$ – see front matter © 2007 Elsevier B.V. All rights reserved.
doi:10.1016/j.jnnfm.2007.10.011

glycol) (PPG) have been investigated in the last years through a number of state-of-the-art experimental techniques such as neutron scattering (NS) [1–6], dielectric spectroscopy [7–13], creep and recoverable compliance measurements [14,15] and time resolved optical spectroscopy[16,17]. Most of these measurements indicate that temperature and pressure exert a stronger influence on segmental relaxation than on terminal relaxation, leading to a crossing of the characteristic curves describing the local and chain relaxation times either at a low enough temperature or at a high enough pressure.

Motivated by these experimental reports, we recently undertook a systematic study [18,19] of the effects of temperature and pressure on structural, thermodynamic and relaxation properties of model *cis*-1,4-polybutadiene (*cis*-1,4-PB) systems by performing long atomistic molecular dynamics (MD) simulations over a wide range of conditions (temperatures ranging from 430 to 195 K, and pressures ranging from 1 atm up to 3 kbar). Segmental or local relaxation was investigated in terms of the dipole moment time autocorrelation function along the *cis*-1,4-PB chain while chain or terminal relaxation was probed by analyzing the time autocorrelation function of the chain end-to-end unit vector. These studies allowed us to reproduce the dielectric loss spectrum of *cis*-1,4-PB under isothermal and isobaric conditions, by Fourier transforming the computed dipole moment time autocorrelation function with respect to time. It was further verified that the temperature dependence of the correlation times characterizing segmental relaxation in *cis*-1,4-PB follows a Vogel–Fulcher–Tammann (VFT) behavior while an Arrhenius-type of equation describes better their pressure dependence [7–11], in accordance with other simulation studies [20–21] and experimental measurements [8,10,15,22–28]. However, and in contrast to what is experimentally observed for other polymers such as PI [7,11,29–31], these MD studies indicated that segmental and chain relaxations in *cis*-1,4-PB are influenced similarly by temperature and pressure variations in the regime of temperature and pressure conditions accessed in the MD simulations (temperatures as low as 195 K and pressures as high as 3 kbar).

The present work complements these studies by extending the MD simulations for a model C_{128} *cis*-1,4-PB system to somewhat lower temperatures (down to 165 K) and by analyzing also: (a) the time autocorrelation function of each Rouse mode [32] $\mathbf{X}_p$ along the simulated C_{128} *cis*-1,4-PB chain, and (b) the coherent [33–35] and incoherent [36,37] dynamic structure factors for different values of the magnitude q of the wavevector. Our results for the incoherent dynamic structure factor are then directly compared with available data obtained from NS measurements for the dependence of the incoherent relaxation times on q. These data [1,4,38–41] support that for values of q corresponding to intermediate length scale dynamics, the relaxation times scale as $\tau \sim q^{-2/\beta}$ where β is the stretching exponent of the Kohlrausch–Williams–Watts (or KWW) function describing the dependence (for a given value of q) of the incoherent dynamic structure factor on time. However, as the magnitude q of the wavevector increases, the scaling of the relaxation times changes to $\tau \sim q^{-2}$. The different scaling of the relaxation times in the low and high q regimes is explained in the literature in terms of the idea of heterogeneous and homogeneous dynamics [42–44]: the existence of distinguishable spatial regions in the system gives rise to the appearance of different relaxation behaviors whose superposition is believed to be responsible for the KWW character of the corresponding structural relaxation.

The heterogeneous dynamical behavior is usually linked with the Gaussian or non-Gaussian character of the Van Hove correlation function [37,39] describing the self-motion of hydrogen atoms in the polymer under study. For example, recent simulation studies and incoherent NS experimental data for PI [39,40] support the transition from a homogenous (i.e., Gaussian in character) dynamical behavior to a heterogeneous (i.e., non-Gaussian in character) one in the region of q values where the static structure factor presents its first peak. NS measurements have also been carried out on PB and PIB samples by Frick et al. [4] under different pressure conditions, and the transition from a homogeneous to a heterogeneous dynamical region was again observed. The experimental measurements of Frick et al. [4] also indicated that the heterogeneous region becomes wider as the pressure increases.

Since details of our MD simulation methodology have been already presented in Refs. [18,19], they will not be repeated here. We only mention that in the present paper, our MD simulations with the C_{128} *cis*-1,4-PB system have been extended to temperatures down to 165 K and, in some cases, to somewhat higher pressures (3.5 kbar). Also, in the case of the lower temperatures studied, we allowed our simulations to run for very long times (up to 2.5 μs in some cases), which helped us get reliable predictions for the relaxation of the normal modes as a function of temperature. The rest of the paper is organized as follows: Section 2 reports our MD results on the Rouse time relaxation spectrum along different isobaric and isothermal conditions. In Section 3, we present results from the analysis of the single chain intermediate coherent dynamic structure factor, $S_{coh}(q, t)$, over the entire range of the simulated temperature and pressure conditions. Additional results for the incoherent intermediate dynamic structure factor, $S_{inc}(q, t)$, are presented in Section 4, supporting the existence of a transition from a homogeneous to a heterogeneous dynamic behavior. Section 5 presents our MD predictions for the characteristic relaxation times of the Rouse modes of the simulated system as a function of temperature and how they can be exploited in the framework of the Rouse model in order to estimate the zero shear rate viscosity of *cis*-1,4-PB (also to verify its fragile character). The paper concludes with Section 6 presenting a summary of the major findings of the present simulation study.

2. The Rouse-mode relaxation spectrum

Parts a and b of Fig. 1 present typical plots of the time autocorrelation function $\langle \mathbf{X}_p(t)\cdot\mathbf{X}_p(0)\rangle/\langle \mathbf{X}_p(0)^2\rangle$ corresponding to the 4th and 8th normal coordinate $\mathbf{X}_p$ of the Rouse model [32] ($p=4$ and 8), respectively, as obtained from the present atomistic MD simulations along different isothermal or isobaric paths, in a linear-log plot. According to the Rouse model, the

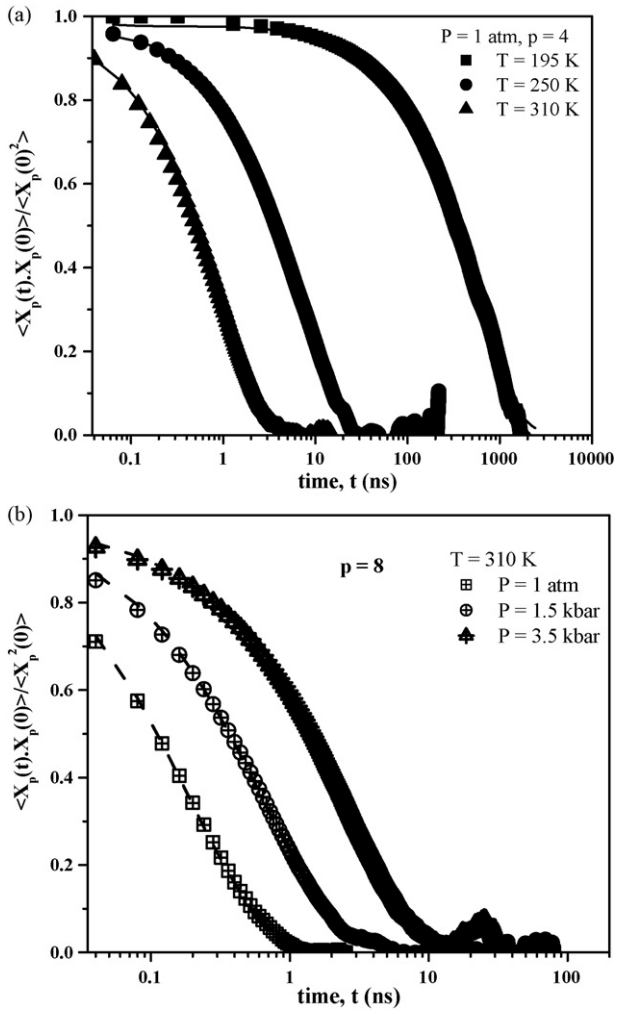

Fig. 1. Time autocorrelation function of: (a) normal mode $p=4$ at different temperatures along an isobar, and (b) normal mode $p=8$ at different pressures along an isotherm, as obtained from the present MD simulations with the C_{128} *cis*-1,4-PB system. The lines represent the best fits to the simulation data with a KWW function, Eq. (3) in the main text.

normal coordinates $\mathbf{X}_p$, $p=0, 1, 2, \ldots, N-1$, are defined as

$$\mathbf{X}_p = \sum_{n=1}^{N} \Omega_{np} \mathbf{R}_{n-1} \tag{1}$$

where Ω_{np} are the elements of the orthogonal matrix $\mathbf{\Omega}$ given by

$$\Omega_{np} = \sqrt{\frac{2-\delta_{p0}}{N}} \cos\left(\frac{((n-1)/2)p\pi}{N}\right) \tag{2}$$

and $\mathbf{R}_n(t)$, $n=1, 2, \ldots, N$, the position vector of the n-th chain bead along the chain. Each $\mathbf{X}_p$ represents the dynamics of the chain which includes N/p segments. As shown in Fig. 1, the obtained simulation curves are accurately fit with stretched exponential (or KWW) functions of the form:

$$\langle \boldsymbol{X}_p(t) \cdot \boldsymbol{X}_p(0)\rangle / \langle X_p^2(0)\rangle = A(p) \exp\left(-\left(\frac{t}{\tau_{\mathrm{KWW}}^p}\right)^{\beta^p}\right) \tag{3}$$

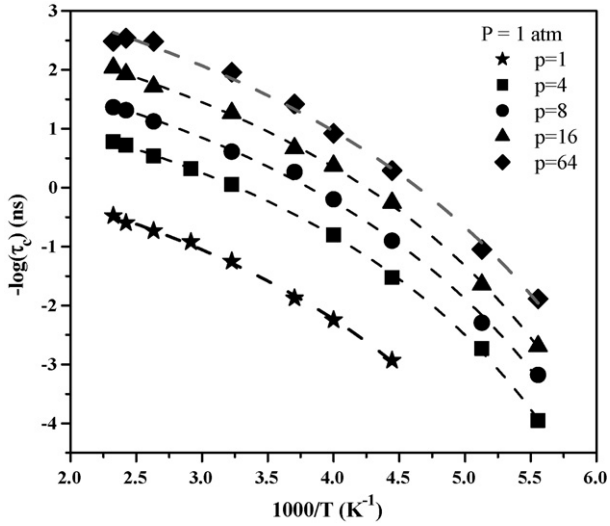

Fig. 2. Temperature dependence of the relaxation time τ_c^p for different Rouse modes, as obtained from the present MD simulations (symbols) with the C_{128} *cis*-1,4-PB system. The lines denote the best fits to the simulation data with a VFT function, Eq. (5) in the main text.

with τ_{KWW}^p and β^p being the characteristic relaxation time and stretching exponent parameters, respectively, and $A(p)$ the amplitude; the latter is introduced in order to account for the fast relaxation of the normal modes at subpicosecond time scales ($t<1$–2 ps), and its best-fit value was found to be a number between 0.8 and 1. The stretching parameter β^p was observed to vary not only with T and P but also with p: in agreement with previous MD simulations [18,34,45], its value increases with increasing temperature or decreasing pressure, and decreases with increasing p (corresponding to more localized motions). For example, at $T=310$ K and $P=1$ atm, β^p decreases from 0.85 to 0.54 as p increases from 1 to 64.

From the fitted τ_{KWW}^p and β^p values, one can calculate the total correlation time, τ_c^p, characterizing the relaxation of the p-th normal mode through:

$$\tau_c^p = \frac{\Gamma(1/\beta^p)}{\beta^p} \tau_{\mathrm{KWW}}^p \tag{4}$$

whose variation with temperature (at $P=1$ atm) for a number of p values is shown in Fig. 2. As p increases, the normal mode describes the dynamics of a shorter part along the C_{128} *cis*-1,4-PB chain; thus, the relaxation times presented in Fig. 2 cover the entire range of length scales: the terminal relaxation (obtained for $p=1$), the relaxation at intermediate length scales (corresponding to p values equal to 4, 8, and 16), and the segmental relaxation (obtained for $p=32$ or 64). The dashed lines shown in the same figure indicate that, for all normal modes p, the temperature dependence of τ_c^p is captured quite well by a modified VFT function [46]:

$$\tau_c^p = \tau_0^p \exp\left(\frac{D^p T}{T - T_0^p}\right) \tag{5}$$

Here, D^p is a dimensionless parameter and T_0^p a characteristic temperature also known as the "ideal" glass transition or Vogel

Table 1
Values of the VFT equation parameters that best fit the simulation results for the normal mode relaxation, Eq. (5) in the main text

Normal mode, p	$\log(\tau_0^p)$ (ns)	D^p	T_0^p (K)
1	5.25 ± 0.20	−4.4 ± 0.4	106 ± 8
4	5.05 ± 0.05	−3.1 ± 0.1	114 ± 2
8	6.02 ± 0.05	−3.4 ± 0.1	114 ± 2
16	6.75 ± 0.05	−3.5 ± 0.1	114 ± 2
24	7.22 ± 0.05	−3.7 ± 0.1	110 ± 2
32	7.44 ± 0.05	−3.8 ± 0.1	109 ± 2
64	7.83 ± 0.05	−3.9 ± 0.1	109 ± 2

temperature. Table 1 lists the best-fit numerical values of τ_0^p, D^p and T_0^p as a function of normal mode number p.

According to several experimental studies with different polymer systems, the temperature dependencies of their segmental and terminal relaxation are indeed described by a VFT function [14,15,27]. However, the experimental data also indicate that the two relaxation times should "freeze" at different Vogel temperatures, so their curves should cross at a temperature somewhat higher than the glass transition temperature (T_g). Consistently with our previous simulation studies [18], but in contrast to these observations for other polymers, the curves shown in Fig. 2 and the reported data in Table 1 support that (in the temperature range covered by the present MD simulations) temperature exerts almost the same influence on all relaxation times (terminal, intermediate and segmental) along a *cis*-1,4-PB chain. On the other hand, the estimated T_0^p values in Table 1 imply that the normal coordinates characterizing intermediate length scales ($p = 4, 8, 16$) should "freeze" at $T_0^p = (114 \pm 2)$ K, a value which decreases somewhat (it drops to (109 ± 2) K) as p increases. This does indicate a somewhat lower "freezing" temperature for the segmental relaxation as compared to less localized motions but the difference is too small to support that the curves of the corresponding relaxation times will certainly cross at a temperature higher than the glass transition temperature (T_g) of the simulated *cis*-1,4-PB system.

Fig. 3 presents the pressure dependence of the relaxation times along two different isothermal paths (corresponding to $T = 310$ K in Part a, and to $T = 413$ K in Part b of the figure), in a log-linear plot. Results are again presented for a number of p values covering all characteristic length scales (from the end-to-end to the monomer scale). The calculated relaxation times τ_c^p are observed to increase exponentially with increasing pressure. Such a dependence, which is in excellent agreement with experimental observations [7–10,16,30], allows us to extract a prediction for the corresponding activation volume ΔV^p through

$$\Delta V^p = 2.303RT\left(\frac{\partial \log(\tau_c^p)}{\partial P}\right)_T \quad (6)$$

and analyze its dependence on normal mode number p under different isothermal conditions. The results obtained (see also Table 2) show that, for a given temperature, the value of ΔV^p is practically insensitive to the p value, except perhaps for the highest ($p = 64$) mode, suggesting a somewhat smaller pressure effect on the segmental relaxation. So, overall, we can say that in

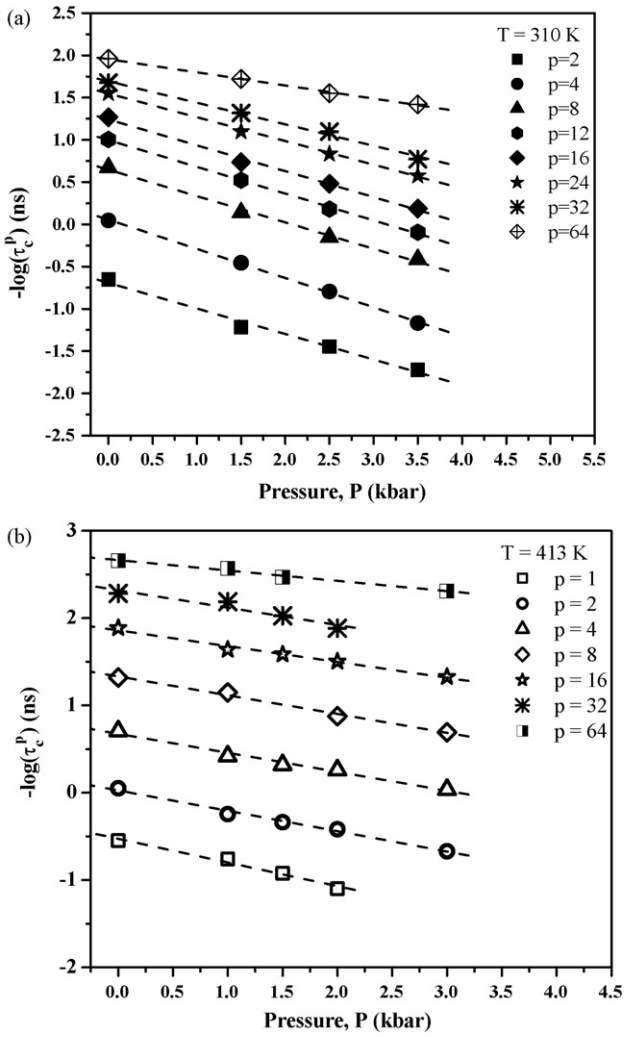

Fig. 3. Pressure dependence of the relaxation time τ_c^p for different Rouse modes, as obtained from the present MD simulations (symbols) with the C_{128} *cis*-1,4-PB system at: (a) $T = 310$ K and (b) $T = 413$ K. The dashed lines represent the best exponential fits to the simulation data.

the range of pressures covered in these MD simulations [1 atm, 3.5 kbar], pressure exerts almost the same influence on the entire normal mode relaxation spectrum. On the other hand, ΔV^p is seen to increase with decreasing temperature, which agrees with

Table 2
Computed values of the activation volume ΔV^p for different Rouse modes, at two different temperatures

ΔV^p (cm^3 mol^{-1})		Normal mode, p
$T = 310$ K	$T = 413$ K	
–	19.5 ± 1.5	1
20.0 ± 0.5	18.5 ± 0.5	2
20.5 ± 0.5	17.5 ± 0.5	4
18.5 ± 0.5	17.0 ± 0.5	8
19.0 ± 0.5	17.5 ± 0.5	12
16.7 ± 0.5	14.8 ± 0.5	16
15.3 ± 0.5	15.0 ± 0.5	24
15.0 ± 0.5	14.8 ± 0.5	32
9.2 ± 0.5	9.6 ± 0.5	64

reported literature data [7]. Furthermore, the values extracted from our MD simulations here are noticeably larger than those reported in Ref. [18] but in very good agreement with the values of ΔV^p [35–19 $cm^3\ mol^{-1}$] reported by Kirpatch and Adolf [16] for *cis*-1,4-PB samples in the temperature range [303–323 K].

3. Single-chain intermediate coherent dynamic structure factor, $S_{coh}(q, t)$

Neutron scattering experimental techniques probe the relaxation of chain-like systems through measurements of the dynamic structure factor $S(q, t)$ of the system [32,37] defined according to

$$S(q,t) \equiv \frac{1}{N}\sum_{n,m}\langle \exp[i\mathbf{q}\cdot(\mathbf{R}_n(t)-\mathbf{R}_m(0))]\rangle \quad (7)$$

where $\mathbf{q}$ denotes the scattering vector whose magnitude is equal to $q=(4\pi/\lambda)\sin(\theta/2)$ where λ is the wavelength of the radiation and θ the scattering angle, and $\mathbf{R}_n(t)$ the position vector of chain segment n along the chain at time t. From Eq. (7) it is obvious that one can explore the entire spectrum of relaxation times for a given polymer by changing the magnitude q of the scattering vector $\mathbf{q}$: small q values (usually $0.01 \le q \le 0.1$ Å^{-1}) probe the overall chain (or terminal) relaxation, while larger q values (usually $1 \le q \le 5$ Å^{-1}) probe the dynamics at shorter length scales (segmental or local relaxation).

MD simulation results are directly comparable to available NS data since the vector $\mathbf{R}_n(t)$–$\mathbf{R}_m(0)$ that appears in Eq. (7) is readily available from the atomistic MD runs. Following the methodology described in Refs. [33,34], the normalized single-chain coherent dynamic structure factor $S_{coh}(q, t)$ is obtained through:

$$S_{coh}(q,t) = \frac{S(q,t)}{S(q,0)} = \frac{\sum_{n,m}\sin[qR_{nm}(t)]/qR_{nm}(t)}{\sum_{n,m}\sin[qR_{nm}(0)]/qR_{nm}(0)} \quad (8)$$

where R_{nm} denotes the magnitude of the vector $\mathbf{R}_n(t)$–$\mathbf{R}_m(0)$ with $n \neq m$. $S_{coh}(q, t)$ has been calculated for a wide range of q values ranging from 0.1 to 3.5 Å^{-1}, corresponding to *cis*-1,4-PB relaxation over all possible length scales (terminal, intermediate and local). Fig. 4 presents the obtained $S_{coh}(q, t)$ curves for $q=0.4$ at $T=413$ K, and for two different pressures ($P=1$ atm and 3 kbar). The dashed lines in the same figure denote the best fits to the $S_{coh}(q, t)$ data with a KWW function:

$$S_{coh}(q,t) = A_{coh}(q)\exp\left(-\left(\frac{t}{\tau^q_{KWW,coh}}\right)^{\beta^q_{coh}}\right) \quad (9)$$

where again $A_{coh}(q)$, $\tau^q_{KWW,coh}$ and β^q_{coh} denote the corresponding characteristic amplitude, relaxation time and stretching exponent parameters, respectively. Consistently with the values of β^p extracted in Section 2 from the KWW fits to the time decay of the autocorrelation functions for the normal modes, the values of β^q_{coh} are found to change smoothly with pressure, showing also a tendency to decrease with increasing q. For example, for

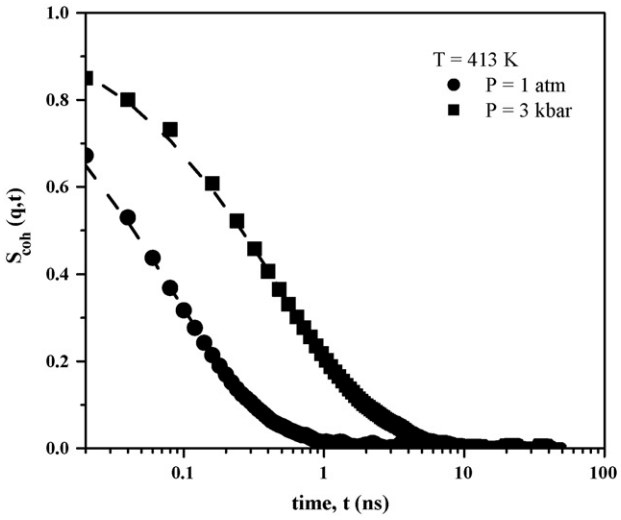

Fig. 4. Plots of the normalized single-chain intermediate coherent dynamic structure factor, $S_{coh}(q, t)$, as obtained from the present MD simulations (symbols) for $q=0.4$ Å^{-1} at two different pressures (1 atm and 3 kbar) along an isotherm ($T=413$ K). The dashed lines represent the best fits to the simulation data with a KWW function, Eq. (9) in the main text.

$T=413$ K and $P=3$ kbar, the value of β^q_{coh} decreases from 0.70 to 0.45 as q increases from 0.2 to 2.0. These values are similar to those calculated by Smith et al. [21] for a random 1,4-PB copolymer sample by fitting MD simulation results for $S_{coh}(q, t)$ also with a KWW function. More precisely, the value 0.617 ± 0.012 at $q=1.44$ Å^{-1} is very close to the value 0.65 ± 0.01 obtained here for $q=1.4$ Å^{-1}, at $T=413$ K and $P=1$ atm.

Fig. 5, on the other hand, shows the variation of the total (correlation) time, $\tau_c^{coh}(q)$, corresponding to a particular q value (as extracted from an equation similar to Eq. (4) above) with pressure, at $T=413$ K. Results are shown in the figure for: $q=0.2$ Å^{-1} (corresponding to terminal relaxation), $q=0.3$–1.0 Å^{-1} (corresponding to the relaxation of intermediate length scales), and $q>1.0$ Å^{-1} (corresponding to segmental

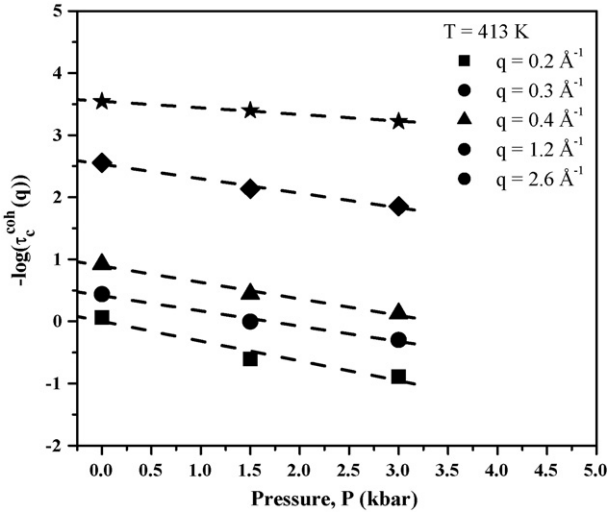

Fig. 5. Pressure dependence of the relaxation time τ_c^{coh} for different q values, at $T=413$ K (symbols). The dashed lines correspond to the best exponential fits to the simulation data.

Table 3
Computed values of the activation volume ΔV^q for different wavevectors q, at $T = 413$ K

q (Å^{-1})	ΔV^q (cm^3 mol^{-1})
0.2	23.0 ± 0.5
0.3	19.5 ± 0.5
0.4	20.5 ± 0.5
1.0	21.0 ± 0.5
1.2	18.5 ± 0.5
1.8	16.5 ± 0.5
2.6	9.0 ± 0.5

relaxation). The computed relaxation times $\tau_c^{coh}(q)$ are found to increase exponentially with increasing pressure, with characteristic activation volume ΔV^q values (obtained though a direct application of Eq. (6)) as listed in Table 3 (at $T = 413$ K). A direct comparison with the data of Table 2 for the relaxation spectrum of the Rouse times confirms again that pressure exerts practically the same influence on all characteristic relaxation times. We also observe that in the temperature range between 310 and 430 K, and independently of the magnitude of the wavevector q considered, ΔV^q increases with decreasing T. For example, for $q = 0.4$ Å^{-1}, its value increases from (17 ± 1) to (24 ± 1) cm^3 mol^{-1} as the temperature is decreased from 430 K down to 310 K, in excellent agreement with reported experimental data in the literature [16].

4. Single-chain intermediate incoherent dynamic structure factor, $S_{inc}(q, t)$

As already mentioned above, recent NS measurements [38–41] have indicated that when the self-motion of the protons in a polymer chain is studied over an extended range of q values, a crossover from a Gaussian to a non-Gaussian dynamic behavior is observed. Indeed, for q values approximately less than 1 Å^{-1}, the relaxation times are measured to scale as $\tau_c^{inc}(q) \propto q^{-2/\beta_{inc}^q}$ (where β_{inc}^q is the stretching exponent of the corresponding KWW function) in accordance with the Gaussian picture of chain relaxation. However, as the range of wavevectors q is extended to larger values (>1.5 Å^{-1}) probing more localized motions, a change in the slope is observed with the relaxation times following a different scaling law: $\tau_c^{inc}(q) \propto q^{-2}$. The crossover is located in the region of wavevectors where the static structure factor $S(q)$ presents its first or intermolecular peak (for most polymers, this is at about 1–1.5 Å^{-1}) and it is attributed to a dynamical heterogeneity, according to which, the presence of spatially localized fast and slow regions gives rise to different, dynamically distinguishable behaviors[43,44,47]. Deviations from the Gaussian form of the self-part of the van Hove correlation function are often used as evidence for such a dynamical heterogeneity.

Theoretically, incoherent NS data are analyzed in terms of the intermediate single chain incoherent scattering function, $S_{inc}(q, t)$, obtained by taking $n = m$ in Eq. (7):

$$S_{inc}(q, t) \equiv \frac{1}{N} \sum_n \langle \exp[i\mathbf{q} \cdot (\mathbf{R}_n(t) - \mathbf{R}_n(0))] \rangle \quad (10)$$

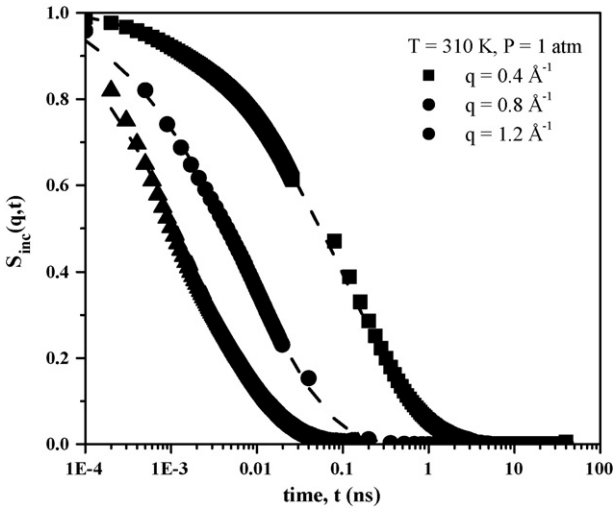

Fig. 6. Plots of the normalized intermediate incoherent dynamic structure factor, $S_{inc}(q, t)$, as obtained from the present MD simulations (symbols) for different q values, at $P = 1$ atm and $T = 310$ K. The dashed lines represent the best fits to the simulation data with a KWW function, Eq. (9) in the main text.

Due to the different scattering cross sections of hydrogen and carbon atoms present in the system, what is actually measured in incoherent NS experiments is the self-motion of the protons. This means that a direct comparison of MD simulation results and incoherent NS experiments is possible only if hydrogen atoms are explicitly present in the MD trajectories. Since our atomistic model is a united-atom one, to make such a comparison possible hydrogen atoms should be explicitly considered; this can be done by a posteriori placing them at their correct positions along the chain backbone following (for example) the methodology outlined in Ref. [34]. Typical plots of the $S_{inc}(q, t)$ functions extracted by such a methodology are reported in Fig. 6. The results have been obtained for three values of the wavevector q (= 0.4, 0.8 and 1.2 Å^{-1}) at $T = 310$ K and $P = 1$ atm, by means of Eq. (10) for each hydrogen in the simulated system. Similarly to the $S_{coh}(q, t)$ curves, the decay of the $S_{inc}(q, t)$ curves is described quite accurately by a KWW function of the form of Eq. (9); Eq. (4) can then be used to compute the corresponding correlation times $\tau_c^{inc}(q)$. Here, it is important to note that, in most experimental studies, the value of the stretching exponent β_{inc}^q used to fit the obtained spectra is taken to remain constant for all q values explored; for example, Frick et al. [4] fitted NS data with a KWW function by considering β_{inc}^q to be fixed, equal to 0.45 (a value also close to other NS and DS experiments). Here, we allowed β_{inc}^q to vary with q in order to optimize the KWW fits of our MD data; the results obtained are discussed in Fig. 7 where the parameter β_{inc}^q is plotted against q for two different pressures ($P = 1$ atm and 1.5 kbar) along an isotherm ($T = 430$ K). Clearly, β_{inc}^q varies significantly with q [36,48,49]. The data presented in Fig. 7 also indicate that upon increasing the pressure, the value of β_{inc}^q decreases slightly.

The dependence of the total correlation time τ_c^{inc} on q under different isothermal and isobaric conditions is shown is Fig. 8. Part a of the figure depicts the variation of τ_c^{inc} with temperature along an isobar, while Part b presents the variation of τ_c^{inc}

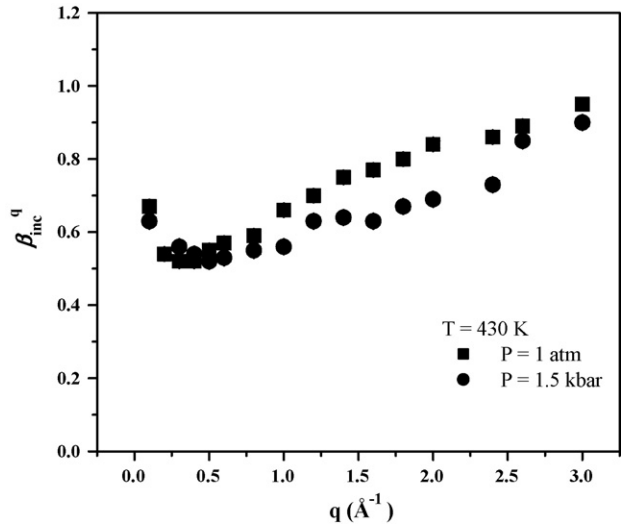

Fig. 7. Variation of the fitting parameter $\beta_{\rm inc}^{q}$ with the wavevector q as obtained from the best fits of the simulated $S_{\rm inc}(q, t)$ curves with a KWW function.

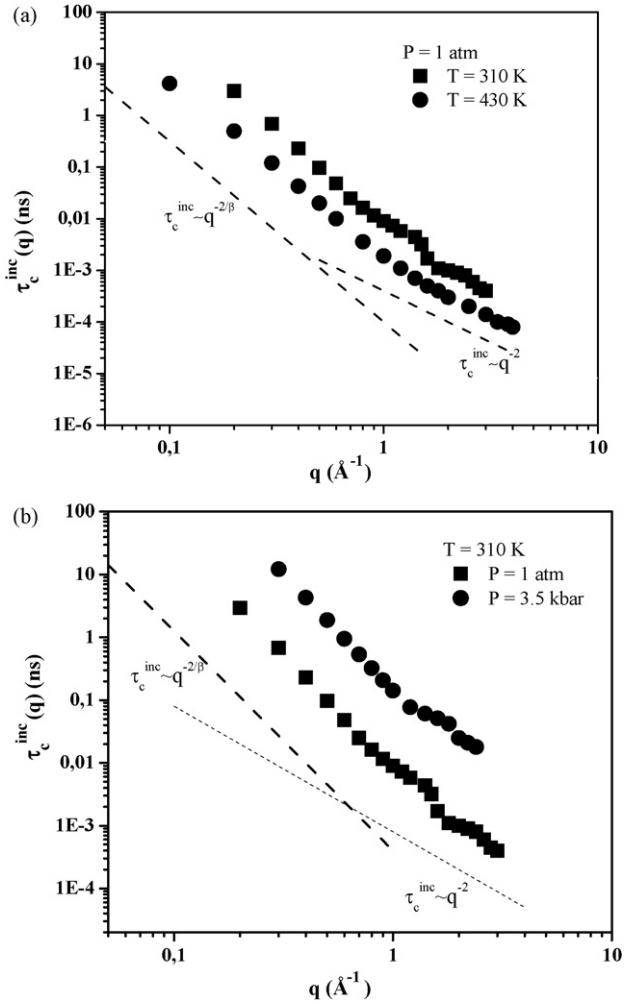

Fig. 8. q dependence of the relaxation time $\tau_{\rm c}^{\rm inc}$ as obtained from the present MD simulations (symbols) at: (a) two different temperatures along an isobar, and (b) two different pressures along an isotherm. The dashed lines serve as guides for the eye to depict the regions were $\tau_{\rm c}^{\rm inc}(q) \propto q^{-2/\beta_{\rm inc}^{q}}$ and $\tau_{\rm c}^{\rm inc}(q) \propto q^{-2}$, respectively.

with pressure along an isotherm, in a log–log plot. The dashed lines in the figure correspond to the power laws $\tau_{\rm c}^{\rm inc}(q) \propto q^{-2}$ (high q region) and $\tau_{\rm c}^{\rm inc}(q) \propto q^{-\gamma}$ (low q region) and have been added as guides for the eye. The parameter γ shown in the latter scaling corresponds to $\gamma = 2/\langle\beta_{\rm inc}\rangle$, with $\langle\beta_{\rm inc}\rangle$ denoting the average value of $\beta_{\rm inc}^{q}$ in the low and intermediate length scales ($\langle\beta_{\rm inc}\rangle \approx 0.55 \pm 0.60$, depending on the temperature and pressure conditions).

Our simulation results are clearly in support of the transition observed in NS experimental measurements from a dynamically homogeneous region in the low q to a dynamically heterogeneous one in the high q region. In all cases, the transition is located near 1.2–1.4 Å^{-1}, which is exactly the regime of wavevectors where the first peak shows up in the $S(q)$ versus q plot for the simulated *cis*-1,4-PB system and the given temperature and pressure conditions (see, e.g., Figs. 12 and 16 of Ref. [19]).

In a recent experimental study, Frick et al. [4] observed that the region of the heterogeneous dynamical behavior is becoming wider as the pressure is increased. This is not entirely obvious in Fig. 8b here, but clearly additional MD simulations at considerably higher pressures are needed to elucidate this point further.

5. Chain relaxation and zero shear rate viscosity

According to the prediction of the Rouse theory [32], the relaxation times corresponding to each normal mode p should scale with p as $\tau_p = \tau_1/p^2$ where $\tau_1 (=\tau_{\rm R})$ is the Rouse or longest chain relaxation time. Fig. 9 depicts how the ratio of $p^2 \cdot \tau_p/\tau_1$ scales with p. The relaxation times τ_p have been calculated through the procedure explained in Section 2; i.e., they correspond to correlation times $\tau_{\rm c}^{p}$ defined through Eqs. (3) and (4). If the Rouse scaling is true then all curves shown in Fig. 9 should fall on the same line corresponding to $p^2 \cdot \tau_{\rm p}/\tau_1 = 1$. The situation is a little different: our MD-based computed relaxation

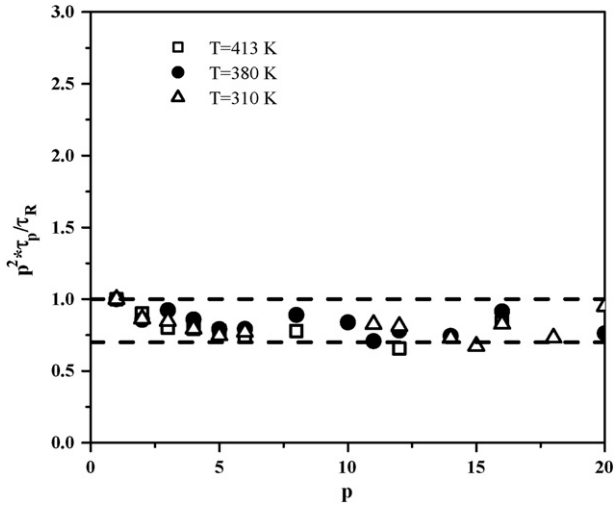

Fig. 9. Scaling of $p^2 \cdot \tau_p/\tau_1$ with mode number p as extracted from our MD simulations at different temperatures. The lines correspond to the cases where $p^2 \cdot \tau_p/\tau_1 = 1$ (based on the formal Rouse theory), and $p^2 \cdot \tau_p/\tau_1 = 0.7$.

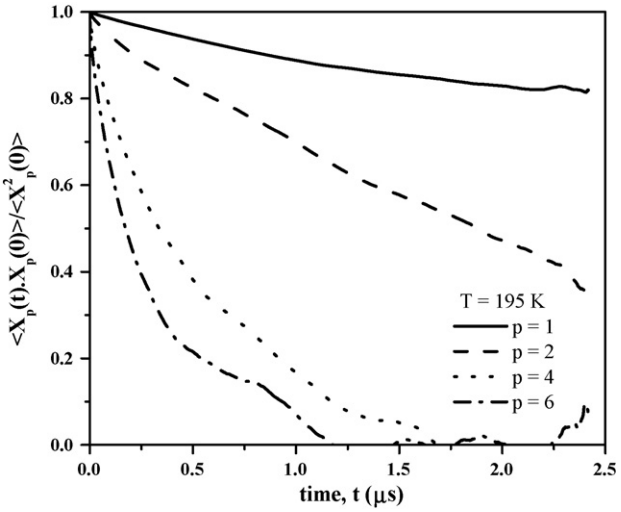

Fig. 10. Decay of the time autocorrelation function $\langle \mathbf{X}_p(t)\cdot\mathbf{X}_p(0)\rangle/\langle \mathbf{X}_p(0)^2\rangle$ for the modes with $p = 1$, 2, 4 and 6, at $T = 195$ K and $P = 1$ atm.

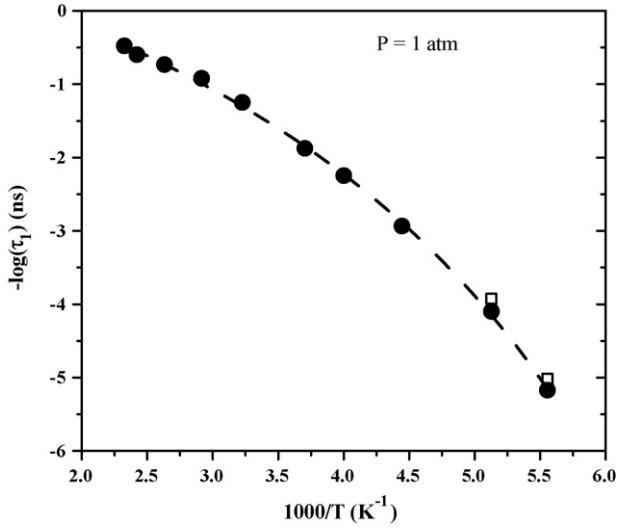

Fig. 11. Temperature dependence of the longest (Rouse) relaxation mode, τ_1, as obtained from the present MD simulations with the C_{128} *cis*-1,4-PB system. For temperatures $T > 225$ K, the values τ_1 have been obtained directly from the decay of the time autocorrelation function for the 1st mode. For temperatures $T < 225$ K, the values of τ_1 have been obtained indirectly from the decay of the time autocorrelation function of the intermediate modes using also that $p^2\cdot\tau_p/\tau_1 = 0.7$ (closed symbols). The two open symbols are the estimates for τ_1 based on the scaling of the formal Rouse theory (namely that $p^2\cdot\tau_p/\tau_1 = 1$ for all mode numbers p). The line denotes the best fit to the simulation data with a VFT function, Eq. (5) in the main text.

times are found to deviate from the Rouse scaling in the sense that the value of the dimensionless quantity $p^2\cdot\tau_p/\tau_1$ depends slightly on mode number p and it is always less than 1. It is interesting, however, to note that overall, $p^2\cdot\tau_p/\tau_1$ attains a constant value equal to 0.7 for all modes (except perhaps for the 2nd or the 3rd), over the entire space of temperatures (above and below the melting point, $T_m = 270$ K) examined. That is, to a very good approximation, the Rouse mode relaxation times as obtained from the KWW fittings of the time autocorrelation functions $\langle \mathbf{X}_p(t)\cdot\mathbf{X}_p(0)\rangle/\langle \mathbf{X}_p(0)^2\rangle$ obey a scaling law of the form $p^2\cdot\tau_p/\tau_1 \cong 0.7$. This is a very significant result because it can be used to extract the Rouse (or longest relaxation) time of the simulated *cis*-1,4-PB system even at temperatures close to the glass transition regime (where τ_1 attains values which are almost three to four orders of magnitude larger than those that can be accessed by MD simulations—a few microseconds in the best case) by observing the relaxation of the higher modes which relax much faster (on time scales that can be tracked by a brute force application of the MD method for a few microseconds, as is the case here). For example, Fig. 10 presents the time decay of the autocorrelation function $\langle \mathbf{X}_p(t)\cdot\mathbf{X}_p(0)\rangle/\langle \mathbf{X}_p(0)^2\rangle$ for $p = 1$, 2, 4 and 6 at $T = 195$ K and $P = 1$ atm. Clearly, in the time span of the MD simulation (2.5 μs), the relaxation of coordinates with $p = 1$ and 2 is incomplete; however, that of the coordinates with $p = 4$ and 6 is complete (the corresponding values of $\langle \mathbf{X}_p(t)\cdot\mathbf{X}_p(0)\rangle/\langle \mathbf{X}_p(0)^2\rangle$ for these modes indeed fall to zero after 2.5 μs). Then, by using, $p^2\cdot\tau_p/\tau_1 \cong 0.7$, one can get a reliable prediction for τ_1. Such a methodology is more accurate to follow compared to the usual practice in the literature (where one tries to get a prediction for τ_1 by extrapolating directly the function $\langle \mathbf{X}_p(t)\cdot\mathbf{X}_p(0)\rangle/\langle \mathbf{X}_p(0)^2\rangle$ for $p = 1$ to zero, which can lead to totally erroneous estimates for τ_1) and should be preferred.

Following the above methodology, in Fig. 11 we present the predictions (closed symbols) for the longest relaxation time τ_1 of the *cis*-1,4-PB system, also for temperatures less than 225 K (for temperatures above 225 K, the relaxation times have been calculated directly from our simulation data following the procedure described in Section 2). The two open symbols in the same figure are the estimates that one would have obtained for τ_1 at $T = 195$ and 180 K if the Rouse scaling had been assumed (i.e., if, instead of $p^2\cdot\tau_p/\tau_1 \cong 0.7$, we had assumed that $p^2\cdot\tau_p/\tau_1 = 1$). The corresponding best-fit parameter values of the modified VFT function that the Rouse relaxation times τ_1 should obey (dashed line in Fig. 11) are then obtained to be: $\log(\tau_0) = 5.98 \pm 0.05$ (ns), $D = -4.9 \pm 0.1$, $T_0 = (98 \pm 2)$ K. These should be compared to those obtained by directly analyzing the time decay of the corresponding autocorrelation function at higher temperatures (see Table 1): τ_1 is now predicted to "freeze" at $T_0 = (98 \pm 2)$ K, i.e., at a temperature which is only 6 K lower than what had been predicted before. This is a very interesting result, indicative of the internal consistency of the analysis of our simulation data (with the modified VFT function) on the basis of a reliable procedure for extracting τ_1 at low enough temperatures from the relaxation of the intermediate normal coordinates, which overcomes the inaccuracies of previous approaches (involving dangerous extrapolations of the time autocorrelation function for the first mode itself by several orders of magnitude in time).

The reliable estimation of the Rouse relaxation time at low enough temperatures offers us the opportunity to make also a reliable estimate of a very important rheological parameter, that of the zero shear rate viscosity, η_0, of the simulated polymer. Indeed, according to the Rouse theory, the value of τ_1, controls the value of η_0 for an unentangled polymer (such as the C_{128} *cis*-1,4-PB simulated here) through the following relation [32]:

$$\eta_0 = \frac{\pi^2}{12}\frac{\rho RT}{M}\tau_1 \tag{11}$$

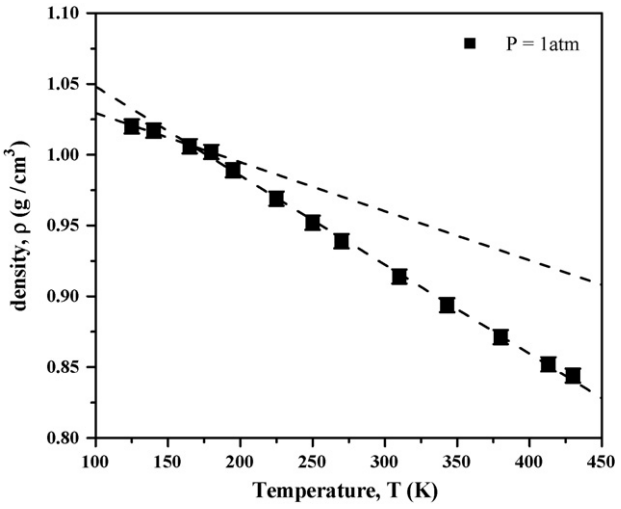

Fig. 12. Temperature dependence of the system density as obtained from our MD simulations with the C_{128} *cis*-1,4-PB system at $P = 1$ atm. The dashed lines represent the best linear fits to simulation data before and after the break in the slope at the lowest temperatures. From the crossing of the two lines the glass transition temperature is estimated to be equal to $T_g = 166$ K.

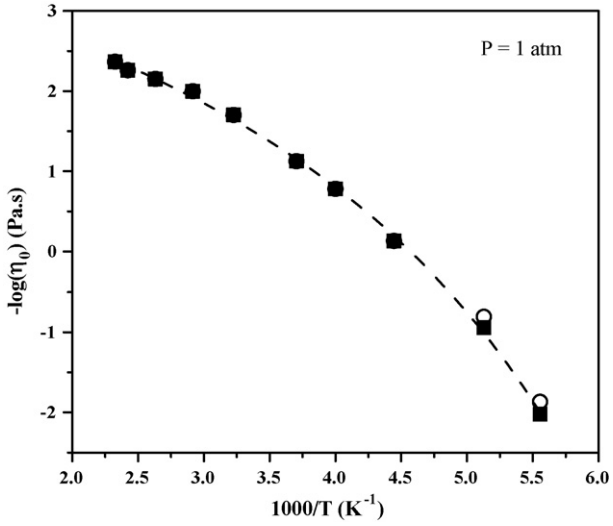

Fig. 13. Temperature dependence of the zero shear rate viscosity η_0 of the simulated C_{128} *cis*-1,4-PB system, as calculated through Eq. (11). Closed symbols represent the values of η_0 extracted by estimating the Rouse relaxation time through $p^2 \cdot \tau_p/\tau_1 = 0.7$. The two open symbols, on the other hand, represent the estimates for η_0 if τ_1 had been calculated according to the Rouse theory scaling, namely that $p^2 \cdot \tau_p/\tau_1 = 1$ for all coordinates p. The dashed line denotes the best fit to the simulation data with a VFT function, Eq. (5) in the main text.

where ρ denotes the system density and M the molecular weight of the unentangled system. The temperature dependence of the density of the simulated system at $P = 1$ atm is shown in Fig. 12. In this plot, we have also included density predictions from additional MD simulation runs at temperatures as low as 125 K. The simulation data depicted in Fig. 12 demonstrate a change in the slope of the line describing the temperature dependence of ρ for a temperature which is around at 166 K; this is the temperature where the glass transition for the simulated *cis*-1,4-PB system should therefore be assigned on the basis of the present MD predictions for the temperature variation of its density.

The corresponding predictions for the zero shear rate viscosity of the simulated C_{128} *cis*-1,4-PB system are illustrated in Fig. 13. The results are shown as a function of the inverse temperature ($1/T$) in a log-linear plot. Also shown in the figure with the open symbols are the estimates that one would have obtained for η_0 at $T = 180$ and 195 K if, instead of $p^2 \cdot \tau_p/\tau_1 \cong 0.7$, we had assumed that $p^2 \cdot \tau_p/\tau_1 = 1$. The temperature dependence of η_0 is captured quite well by a modified VFT function (dashed line in Fig. 13) with best-fit parameter values equal to $\log(\eta_0) = (7.2 \pm 0.01)$ (Pa s), $D = (-3.6 \pm 0.1)$, $T_0 = (110 \pm 1)$ K, indicative of the fragile [50,51] character of the *cis*-1,4-PB polymer. On the basis of rheological experiments, T_g is defined as the temperature where $\eta_0 \approx 10^{12}$ Pa s. According to the data presented in Fig. 13 and the best-fit VFT function parameters, this value for the simulated C_{128} *cis*-1,4-PB system is obtained for a temperature close to 135 K. Based on this result as well as on our prediction for the break in the slope of the temperature variation of the density of the simulated system discussed in the previous paragraph, we conclude that our estimation for the glass transition temperature T_g of the simulated C_{128} *cis*-1,4-PB system is that it lies between 135 and 166 K. This is in excellent agreement with reported literature data for the glass transition temperature of 1,4-PB systems [52,53].

In the literature, a measure of the fragile character of a substance is provided by the fragility index m [54] defined through:

$$m = \left.\frac{d\ \log(\tau_1)}{d(T_g/T)}\right|_{T=T_g} \quad \text{or} \quad m = \left.\frac{d\ \log(\eta_0)}{d(T_g/T)}\right|_{T=T_g} \tag{12}$$

A direct calculation of the fragility index for the C_{128} *cis*-1,4-PB system based on the data presented in Figs. 11 and 13 and the estimate for the glass transition temperature obtained from the temperature dependence of the zero shear rate viscosity (i.e., $T_g \approx 135$ K) gives a value of m equal to 130. In the literature [54,55], typical values for the index m of a number of random copolymer systems of 1,2-PB and 1,4-PB range between 84 and 133 (depending on their composition, i.e., on the relative fraction of *cis* and *trans* content).

6. Summary and conclusions

We have investigated the relaxation behavior of a C_{128} *cis*-1,4-PB system over its complete spectrum of characteristic length scales (terminal, intermediate and segmental) through long, atomistic MD simulations in an extended range of temperature (from 430 K down to 165 K) and pressure (from 1 atm up to 3.5 kbar) conditions. By denoting each CH_2 and CH unit present in the *cis*-1,4-PB system as a different Rouse bead and analyzing the long atomistic MD trajectories at different thermodynamic conditions, we first explored the temperature and pressure dependence of the relaxation times assigned to different Rouse modes. In agreement with experimental observations and other simulation results, the temperature dependence for all modes was seen to follow a VFT behavior while an Arrhenius behavior was seen to describe their pressure dependence. From the slope of the lines representing the pressure dependence of

the Rouse relaxation times, the activation volume ΔV^p was calculated and found to be in remarkable agreement with reported experimental measurements [16].

In a second step, we calculated the single chain intermediate coherent structure factor $S_{coh}(q, t)$ along different isothermal and isobaric conditions. By fitting the simulated curves with a KWW function, a relaxation time was assigned to a number of values of the wavevector q analyzed. From the slope of the curves describing the pressure dependences of this relaxation time, the activation volume ΔV^q was calculated and analyzed as a function of q; ΔV^q was found to be almost identical to the corresponding ΔV^p value from the normal mode analysis.

Our MD simulation results were next compared to available incoherent NS experimental data. To this end, hydrogen atoms were introduced along the chain in the atomistic trajectories and their self-motion was explored through calculations of the single chain incoherent structure factor $S_{inc}(q, t)$ for different q values, and also as a function of temperature and pressure. By fitting the simulated $S_{inc}(q, t)$ curves with a KWW function, the relaxation times corresponding to different q values were computed. By plotting them as a function of q, a transition from a homogeneous to a heterogeneous dynamic behavior was revealed. Consistently with previous studies and experimental measurements, this transition was seen to be located at the region where the static structure factor, $S(q)$, presents its first peak (around 1.2–1.4 $Å^{-1}$) [6,40,56]. The q dependence of the incoherent relaxation times along different isobaric conditions, up to $P = 3.5$ kbar, did not confirm the experimental observation [4] that heterogeneous region is expanded towards lower q values as the pressure is increased.

In the last stage of this work, a methodology was presented which allowed us to extract reliable predictions for the longest or Rouse relaxation time and the zero shear rate viscosity of the simulated system at temperatures around its glass transition region. Our MD simulation results support that the characteristic normal mode spectrum of relaxation times deviates slightly from the scaling formally suggested by the Rouse theory in the sense that the dimensionless ratio $p^2 \cdot \tau_p/\tau_1$ is not equal to 1 for all mode numbers p but depends slightly on p attaining values close to 0.7 for most of the modes. By assuming that the same scaling is also followed at the lowest temperatures, we managed to calculate first the Rouse time and then the zero shear rate viscosity near the glass transition temperature. Both τ_R and η_0 were observed to follow a VFT behavior revealing the fragile character of the *cis*-1,4-PB polymer. An estimation for the fragility index m of the simulated *cis*-1,4-PB system was also reported.

References

[1] B. Frick, C. Alba-Simionesco, Comparison of the pressure and temperature dependence of the elastic incoherent scattering for the polymers polybutadiene and polyisobutylene, Phys. B: Condens. Matter 266 (1999) 13–19.

[2] B. Frick, C. AlbaSimionesco, J. Hendricks, L. Willner, Incoherent inelastic neutron scattering on polybutadiene under pressure, Prog. Theor. Phys. Suppl. 126 (1997) 213–218.

[3] B. Frick, C. Alba-Simionesco, K.H. Andersen, L. Willner, Influence of density and temperature on the microscopic structure and the segmental relaxation of polybutadiene, Phys. Rev. E 67 (2003) 051801-1-15.

[4] B. Frick, G. Dosseh, A. Cailliaux, C. Alba-Simionesco, Pressure dependence of the segmental relaxation of polybutadiene and polyisobutylene and influence of molecular weight, Chem. Phys. 292 (2003) 311–323.

[5] D. Richter, B. Frick, B. Farago, Neutron-spin-echo investigation on the dynamics of polybutadiene near the glass-transition, Phys. Rev. Lett. 61 (1988) 2465–2468.

[6] A. Arbe, J. Colmenero, B. Farago, M. Monkenbusch, U. Buchenau, D. Richter, Intermediate length scale dynamics in glass forming polymers: coherent and incoherent quasielastic neutron scattering results on polyisobutylene, Chem. Phys. 292 (2003) 295–309.

[7] G. Floudas, C. Gravalides, T. Reisinger, G. Wegner, Effect of pressure on the segmental and chain dynamics of polyisoprene. Molecular weight dependence, J. Chem. Phys. 111 (1999) 9847–9852.

[8] M. Mierzwa, G. Floudas, J. Dorgan, D. Knauss, J. Wegner, Local and global dynamics of polylactides. A dielectric spectroscopy study, J. Non-Cryst. Solids 307 (2002) 296–303.

[9] M. Paluch, S. Pawlus, C.M. Roland, Pressure and temperature dependence of the alpha-relaxation in poly(methyltolylsiloxane), Macromolecules 35 (2002) 7338–7342.

[10] C.M. Roland, R. Casalini, T. Psurek, S. Pawlus, M. Paluch, Segmental- and normal-mode dielectric relaxation of poly(propylene glycol) under pressure, J. Polym. Sci. Part B: Polym. Phys. 41 (2003) 3047–3052.

[11] P.G. Santangelo, C.M. Roland, Temperature dependence of mechanical and dielectric relaxation in *cis*-1,4-polyisoprene, Macromolecules 31 (1998) 3715–3719.

[12] Y.F. Ding, A.P. Sokolov, Breakdown of time-temperature superposition principle and universality of chain dynamics in polymers, Macromolecules 39 (2006) 3322–3326.

[13] G. Floudas, K. Mpoukouvalas, P. Papadopoulos, The role of temperature and density on the glass-transition dynamics of glass formers, J. Chem. Phys. 124 (2006) 074905-1-5.

[14] D.J. Plazek, X.D. Zheng, K.L. Ngai, Viscoelastic properties of amorphous polymers. 1. Different temperature dependences of segmental relaxation and terminal dispersion, Macromolecules 25 (1992) 4920–4924.

[15] D.J. Plazek, E. Schlosser, A. Schonhals, K.L. Ngai, Breakdown of the Rouse model for polymers near the glass-transition temperature, J. Chem. Phys. 98 (1993) 6488–6491.

[16] A. Kirpatch, D.B. Adolf, High-pressure study of the local dynamics of melt *cis*-1,4-polybutadiene and *cis*-1,4-polyisoprene, Macromolecules 37 (2004) 1576–1582.

[17] B.J. Punchard, D.B. Adolf, Pressure and temperature dependence of the melt segmental dynamics of *cis*-1,4-polyisoprene via time resolved optical spectroscopy, J. Chem. Phys. 117 (2002) 7774–7780.

[18] G. Tsolou, V.A. Harmandaris, V.G. Mavrantzas, Atomistic molecular dynamics simulation of the temperature and pressure dependences of local and terminal relaxations in *cis*-1,4-polybutadiene, J. Chem. Phys. 124 (2006) 084906-1-11.

[19] G. Tsolou, V.A. Harmandaris, V.G. Mavrantzas, Temperature and pressure effects on local structure and chain packing in *cis*-1,4-polybutadiene from detailed molecular dynamics simulations, Macromol. Theor. Simul. 15 (2006) 381–393.

[20] M. Doxastakis, D.N. Theodorou, G. Fytas, F. Kremer, R. Faller, F. Muller-Plathe, N. Hadjichristidis, Chain and local dynamics of polyisoprene as probed by experiments and computer simulations, J. Chem. Phys. 119 (2003) 6883–6894.

[21] G. Smith, D. Bedrov, W. Paul, A molecular dynamics simulation study of the alpha-relaxation in a 1,4-polybutadiene melt as probed by the coherent dynamic structure factor, J. Chem. Phys. 121 (2004) 4961–4967.

[22] K.L. Ngai, A. Schonhals, E. Schlosser, An explanation of anomalous dielectric-relaxation properties of poly(propylene glycol), Macromolecules 25 (1992) 4915–4919.

[23] K.L. Ngai, D.J. Plazek, S.S. Deo, Physical origin of the anomalous temperature-dependence of the steady-state compliance of low-molecular weight polystyrene, Macromolecules 20 (1987) 3047–3054.

[24] P. Papadopoulos, G. Floudas, I. Schnell, H.A. Klok, T. Aliferis, H. Iatrou, N. Hadjichristidis, "Glass transition" in peptides: temperature and pressure effects, J. Chem. Phys. 122 (2005) 224906-1-4.

[25] K. Mpoukouvalas, G. Floudas, Phase diagram of poly(methyl-*p*-tolylsiloxane): a temperature- and pressure-dependent dielectric spectroscopy investigation, Phys. Rev. E 68 (2003) 031801-1-8.
[26] R. Casalini, C.M. Roland, Temperature and density effects on the local segmental and global chain dynamics of poly(oxybutylene), Macromolecules 38 (2005) 1779–1788.
[27] T. Nicolai, G. Floudas, Dynamics of linear and star poly(oxypropylene) studied by dielectric spectroscopy and rheology, Macromolecules 31 (1998) 2578–2585.
[28] C.M. Roland, R. Casalini, Temperature and volume effects on local segmental relaxation in poly(vinyl acetate), Macromolecules 36 (2003) 1361–1367.
[29] K. Adachi, H. Hirano, Slow dielectric relaxation of *cis*-polyisoprene near the glass transition temperature, Macromolecules 31 (1998) 3958–3962.
[30] G. Floudas, T. Reisinger, Pressure dependence of the local and global dynamics of polyisoprene, J. Chem. Phys. 111 (1999) 5201–5204.
[31] A. Schönhals, Relation between main and normal mode relaxations for polyisoprene studied by dielectric-spectroscopy, Macromolecules 26 (1993) 1309–1312.
[32] M. Doi, S.F. Edwards, The theory of Polymer Dynamics, Clarendon Press, Oxford, England, 1986.
[33] V.A. Harmandaris, V.G. Mavrantzas, D.N. Theodorou, M. Kröger, J. Ramirez, H.C. Öttinger, D. Vlassopoulos, Crossover from the rouse to the entangled polymer melt regime: signals from long, detailed atomistic molecular dynamics simulations, supported by rheological experiments, Macromolecules 36 (2003) 1376–1387.
[34] G. Tsolou, V.G. Mavrantzas, D.N. Theodorou, Detailed atomistic molecular dynamics simulation of *cis*-1,4-poly(butadiene), Macromolecules 38 (2005) 1478–1492.
[35] A. Baumgärtner, U. Ebert, L. Schäfer, The coherent scattering function of the reptation model: simulation compared to theory, Eur. Phys. J. E 12 (2003) 303–319.
[36] F. Ganazzoli, G. Raffaini, V. Arrighi, The stretched-exponential approximation to the dynamic structure factor in non-entangled polymer melts, Phys. Chem. Chem. Phys. 4 (2002) 3734–3742.
[37] J. Higgins, H.C. Benoit, Polymers and Neutron Scattering, Oxford University Press Inc, New York, 1996.
[38] J. Colmenero, A. Arbe, A. Alegria, M. Monkenbusch, D.D Richter, On the origin of the non-exponential behaviour of the alpha-relaxation in glass-forming polymers: incoherent neutron scattering and dielectric relaxation results, J. Phys.: Condens. Matter 11 (1999) A363–A370.
[39] A. Arbe, J. Colmenero, F. Alvarez, M. Monkenbusch, D. Richter, B. Farago, B. Frick, Non-Gaussian nature of the alpha relaxation of glass-forming polyisoprene, Phys. Rev. Lett. 89 (2002), 245701-1-4.
[40] A. Arbe, J. Colmenero, F. Alvarez, M. Monkenbusch, D. Richter, B. Farago, B. Frick, Experimental evidence by neutron scattering of a crossover from Gaussian to non-Gaussian behavior in the alpha relaxation of polyisoprene, Phys. Rev. E 67 (2003), 051802-1-16.
[41] B. Farago, A. Arbe, J. Colmenero, R. Faust, U. Buchenau, D. Richter, Intermediate length scale dynamics of polyisobutylene, Phys. Rev. E 65 (2002), 051803-1-17.
[42] D. Richter, M. Monkenbusch, A. Arbe, J. Colmenero, B. Farago, R. Faust, Space time observation of the alpha-process in polymers by quasielastic neutron scattering, J. Phys.: Condens. Matter 11 (1999) A297–A306.
[43] H. Sillescu, Heterogeneity at the glass transition: a review, J. Non-Cryst. Solids 243 (1999) 81–108.
[44] A. Arbe, J. Colmenero, M. Monkenbusch, D. Richter, Dynamics of glass-forming polymers: "Homogeneous" versus "heterogeneous" scenario, Phys. Rev. Lett. 81 (1998) 590–593.
[45] G.D. Smith, O. Borodin, D. Bedrov, W. Paul, X.H. Qiu, M.D. Ediger, C-13 NMR spin-lattice relaxation and conformational dynamics in a 1,4-polybutadiene melt, Macromolecules 34 (2001) 5192–5199.
[46] P. Papadopoulos, D. Peristeraki, G. Floudas, G. Koutalas, N. Hadjichristidis, Origin of glass transition of poly(2-vinylpyridine). A temperature- and pressure-dependent dielectric spectroscopy study, Macromolecules 37 (2004) 8116–8122.
[47] D. Richter, M. Monkenbusch, J. Allgeier, A. Arbe, J. Colmenero, B. Farago, Y.C. Bae, R. Faust, From Rouse dynamics to local relaxation: a neutron spin echo study on polyisobutylene melts, J. Chem. Phys. 111 (1999) 6107–6120.
[48] A. Neelakantan, J.K. Maranas, Spatial regimes in the dynamics of polyolefins: self-motion, J. Chem. Phys. 120 (2004) 465–474.
[49] G. Arialdi, K. Karatasos, J.P. Rychaert, V. Arrighi, F. Saggio, A. Triolo, A. Desmedt, J. Pieper, R.E. Lechner, Local dynamics of polyethylene and its oligomers: a molecular dynamics interpretation of the incoherent dynamic structure factor, Macromolecules 36 (2003) 8864–8875.
[50] C.A. Angell, K.L. Ngai, P.F. McMillan, S.W. Martin, Relaxation in glass-forming liquids and amorphous solids, J. App. Phys. 88 (2000) 3113–3157.
[51] P.G. Debenedetti, F.H. Stillinger, Supercooled liquids and the glass transition, Nature 410 (2001) 259–267.
[52] W.D. Van Krevelen, Properties of Polymers: Their Estimation and Correlation with Chemical Structure, Elsevier, Amsterdam, 1990.
[53] J.D. Ferry, Viscoelastic Properties of Polymers, J. Wiley & sons, New York, 1980.
[54] R. Böhmer, K.L. Ngai, C.A. Angell, D.J. Plazek, Nonexponential relaxations in strong and fragile glass formers, J. Chem. Phys. 99 (1993) 4201–4209.
[55] C.M. Roland, K.L. Ngai, Segmantal relaxation and molecular structure in polybutadienes and polyisoprene, Macromolecules 24 (1991) 5315–5319.
[56] J. Colmenero, F. Alvarez, A. Arbe, Self-motion and the alpha relaxation in a simulated glass-forming polymer: crossover from Gaussian to non-Gaussian dynamic behavior, Phys. Rev. E 65 (2002), 041804-1-12.